Photoproduction of pseudoscalar mesons on 1*p*-shell nuclei at high energies and forward angles

A. Fix *
Tomsk Polytechnic University, Tomsk 634050, Russia

(Received 20 July 2023; accepted 27 September 2023; published 11 October 2023)

I address the issue of coherent and incoherent photoproduction of pseudoscalar mesons on nuclei at high photon energies in the peripheral region, characterized by small momentum transfer. The reactions considered give prominent background to photoproduction in the electromagnetic field of a nucleus. For this reason, a detailed knowledge of their cross sections is necessary for correct determination of the radiative decay widths of neutral mesons. Particular attention is paid to transitions to the discrete bound levels, as well as to the giant resonance states. Numerical results are presented for photoproduction of η mesons on ^{12}C.

DOI: 10.1103/PhysRevC.108.044607

I. INTRODUCTION

Photoproduction of neutral pseudoscalar mesons in the nuclear Coulomb field (the Primakoff effect) is one of the efficient methods for determining their radiative widths. Recently, the PrimEx collaboration has launched an extensive experimental program at Jefferson Laboratory, aimed at a high precision measurement of the Primakoff cross section in π^0, η, and η' sectors [1,2]. One of the difficulties inherent in such measurements is the necessity of separating the Coulomb mechanism from the background reactions, in which the meson is produced via direct interaction of the incident photon with the target nucleons. Therefore, it is important that the model used for calculating the relevant amplitudes be sufficiently reliable and free from significant quantitative uncertainties.

The theoretical framework, aimed at describing meson photoproduction on a nucleus, separates quite naturally into three basic ingredients: (i) single-nucleon amplitude, (ii) nuclear model, and (iii) final state interaction (FSI), which are of equal importance for reliable theoretical treatment. The earlier calculations [3–5] were, as a rule, based on rather crude nuclear models (typically a uniform nuclear density or a naive shell model were used), as well as on an oversimplified treatment of a single-nucleon amplitude.

In the more recent works the photoproduction mechanism and interaction of the probes with the target nucleons were considered in much more sophisticated framework incorporating the complex many-particle dynamics of these processes. Here, one should mention the Monte Carlo algorithm incorporated in [6]. In much of the theory, the elements of quasiclassical approach, in particular Glauber theory, were used [7–9]. The latter assumes that the produced meson moves in the nucleus along a classical linear trajectory. All nucleons are considered frozen, and their interaction with the traveling meson does not depend on the presence of other surrounding nucleons.

In the peripheral region, where the kinetic energy of the produced meson is high, so that interaction with the nucleus is unable to visibly bend its trajectory, and the momentum transferred to the nucleus is small, the quasiclassical picture is known to work quite successfully.

The essential point is also that at very forward angles the largest contribution usually comes from the elastic (coherent) photoproduction mechanism which is much less subject to model uncertainty than inelastic transitions. For a spin-zero nucleus, the dependence of the coherent cross section on the meson angle θ is predominantly determined by the interplay between the nuclear form factor and the characteristic dependence $\vec{q}\cdot(\vec{k}\times\vec{\varepsilon}_\lambda)$ of the non-spin-flip part of the pseudoscalar photoproduction amplitude. After averaging over the photon polarization λ, the latter gives the factor $\sin^2\theta$, so that the angular dependence of the resulting cross section in the region of low momentum transfer $Q=|\vec{k}-\vec{q}\,|\approx k\,\theta$ is given to a good approximation by

$$\frac{d\sigma}{d\Omega}\sim A^2\sin^2\theta\left(1-\frac{Q^2\langle r^2\rangle}{6}+\cdots\right)^2, \tag{1}$$

where A is the mass number of the target nucleus, and $\langle r^2\rangle^{1/2}$ is its mean square radius. The coefficient in Eq. (1) is basically determined by the single-nucleon cross section. If the latter is well known, the model uncertainty has a minor effect on the results.

The contribution of the incoherent channels into the inclusive cross section, including excitation of the target to discrete levels, as well as transitions to the continuous spectrum (at forward meson angles the latter is mainly determined by single nucleon knock-out) are, as a rule, taken into account via the completeness (closure) relation

$$\sum_f|\langle f|\hat{\mathcal{O}}|i\rangle|^2=\langle i|\hat{\mathcal{O}}^\dagger\hat{\mathcal{O}}|i\rangle. \tag{2}$$

Neglecting the kinematic corrections due to nuclear binding, target excitation, etc., a simple expression for the resulting

*fix@tpu.ru

incoherent cross section can be obtained [3,10] as

$$\frac{d\sigma}{d\Omega} = A\,\frac{d\sigma_N}{d\Omega}[\,1 - G(Q)], \tag{3}$$

where $d\sigma_N/d\Omega$ is the single-nucleon cross section and $G(Q)$ effectively takes into account nuclear correlations. In particular, Pauli exclusion principle requires $G(0) \to 1$ and $G(2P_F) \approx 0$ with P_F being the Fermi momentum.

Although a simplified treatment of the model ingredients (i) to (iii), mentioned above, can be considered reliable in the region of high energies and very forward production angles, it might be instructive to examine closely the role of individual channels within a more sophisticated approach. The importance of this task is due to several reasons. First, it is interesting to trace which background processes make the most significant contributions to the resulting cross section with increasing momentum transfer. Understanding the underlying background mechanisms, beyond an oversimplified prescription like that given by the expression (3), can be useful for an analysis of the corresponding experimental cross sections in the vicinity of the Primakoff maximum. Second, although it might appear at first glance that accounting for a large number of channels is a cumbersome task, such calculations are in fact not very difficult, since the theory of coherent and incoherent meson photoproduction on nuclei is quite well developed. The results obtained in this way can also serve as a good quantitative test of the reliability of the approximations mentioned above.

In the present paper, I calculate, besides the coherent production, also the incoherent channels in which the nucleus is excited to discrete bound-state levels. These include both the low-lying $0\hbar\omega$ excitations and the transitions involving parity change, in particular, the excitation of the giant resonance states.

Since my formalism differs from that used in the above cited works, a significant part of the paper is devoted to the presentation of some of the most important formal ingredients. As a particular example, the photoproduction of η mesons on carbon,

$$\gamma + {}^{12}\mathrm{C} \to \eta + {}^{12}\overset{*}{\mathrm{C}}, \tag{4}$$

is considered, but the formalism is applicable to the general case of photoproduction of spinless mesons on $1p$-shell nuclei. In the next section I present the theoretical framework for evaluation of the elementary η photoproduction operator. The corresponding two-component form is valid for an arbitrary reference frame which is convenient for nuclear applications. The ingredients of the model for $A(\gamma, \eta)A^*$ are presented in Sec. III. In Sec. IV I discuss my results for the reactions on ^{12}C. Conclusions are given in Sec. V.

II. THE ELEMENTARY PHOTOPRODUCTION AMPLITUDE

Throughout the paper the conventions of Bjorken and Drell [11] are used. I start from the photoproduction of η mesons on a free single nucleon

$$\gamma(k^\mu, \lambda) + N_i(p^\mu) \to \eta(q^\mu) + N_f(p'^\mu). \tag{5}$$

Here, λ is the photon polarization index, and the particle four-momenta indicated in the parentheses are

$$k^\mu = (E_\gamma, \vec{k}\,), \quad p^\mu = (E_i, \vec{p}\,),$$
$$q^\mu = (\omega_\eta, \vec{q}\,), \quad p'^\mu = (E_f, \vec{p}\,'). \tag{6}$$

Since the amplitude of the reaction (5) is intended for use in nuclear calculations, to correctly take into account Fermi motion I represent the corresponding single nucleon operator in a form that allows using it in an arbitrary frame of reference. To this end, I follow the prescriptions from Refs. [12,13] where one starts from the Lorentz covariant expression (the isotopic part is omitted for the moment)

$$F = \bar{u}_f(p', m'_s)\left[\sum_{j=1}^{4} A_j(s,t)\hat{M}_j\right]u_i(p, m_s), \tag{7}$$

where $u_i(p, m_s)$ and $u_f(p', m'_s)$ are the Dirac spinors of the initial and final nucleons, $\hat{M}_j$, $j = 1, \ldots, 4$, are the gauge invariant forms composed of the Dirac matrices, photon polarization vector ε_λ, and four-momenta of the participating particles, and A_j are the invariant amplitudes depending on the Mandelstam variables. For M_j I choose the combinations adopted in [14], which were also used in Ref. [12].

The amplitudes A_j are determined, of course, by a particular model used for $\gamma N \to \eta N$. Since I consider here only high energies where the excitation of s-channel baryon resonances is insignificant, and the cross section demonstrates a pronounced diffractive behavior, it is reasonable to parametrize the amplitude in terms of vector meson exchange in the t channel. In this case

$$A_1 = \frac{e\lambda_V}{M_\eta}\left[2M_N g^v_{VNN} + \frac{g^t_{VNN}}{2M_N}\,t\right]G_V(t), \tag{8a}$$

$$A_2 = \frac{e\lambda_V}{M_\eta}\,\frac{g^t_{VNN}}{2M_N}\,G_V(t), \tag{8b}$$

$$A_3 = \frac{e\lambda_V}{M_\eta}\,g^v_{VNN}\,G_V(t), \tag{8c}$$

$$A_4 = A_3 \tag{8d}$$

with M_η and M_N being the η and the nucleon mass, respectively. In the present calculation I use only ω and ρ exchange. The corresponding parameters, the radiative $\gamma\eta V$ couplings λ_V, and the vector and tensor VNN coupling constants g^v_{VNN}, g^t_{VNN} were taken from the analysis of [15]. Furthermore, following [15] I use for the propagators $G_V(t)$ the Regge ansatz with a rotating phase

$$G_V(t) = \left(\frac{s}{s_0}\right)^{\alpha_V(t)-1}\frac{\pi\alpha'_V}{\sin[\pi\alpha_V(t)]}\,\frac{e^{-i\pi\alpha_V(t)}}{\Gamma(\alpha_V(t))}. \tag{9}$$

Here, the mass scale $s_0 = 1$ GeV, and the coefficients α_V, α'_V of the Regge trajectories $\alpha_V(t) = \alpha_V + \alpha'_V\,t$ are given in [15]. All parameters were obtained by fitting the data for $\gamma p \to \eta p$ in the energy region $E_\gamma \leqslant 6$ GeV.

To adopt the operator (7) to the calculation on a nucleus with nonrelativistic wave functions, I turn to the equivalent two-component spin representation in terms of Pauli

spinors χ_{m_s}:

$$\bar{u}_f(p', m_s')\hat{F}\, u_i(p, m_s) = \chi^{\dagger}_{m_s'}\hat{t}_{\eta\gamma}(p', p)\chi_{m_s}. \tag{10}$$

The 2×2 component operator $\hat{t}_{\eta\gamma}$ may be decomposed into the spin-independent and the spin-flip part

$$\hat{t}_{\eta\gamma} = L_\lambda + \vec{K}_\lambda\cdot\vec{\sigma}. \tag{11}$$

Both L and $\vec{K}$ are operators in the isospin space

$$L_\lambda = L_{\lambda(0)} + L_{\lambda(1)}\tau_0, \quad \vec{K}_\lambda = \vec{K}_{\lambda(0)} + \vec{K}_{\lambda(1)}\tau_0 \tag{12}$$

with $\tau_0|p\rangle = |p\rangle$, $\tau_0|n\rangle = -|n\rangle$. In my model, the isoscalar part $L_{(0)}$, $\vec{K}_{(0)}$ for photoproduction of an isoscalar meson (η, η') is due exclusively to the ω trajectory, whereas the isovector part $L_{(1)}$, $\vec{K}_{(1)}$ is determined by the exchange of the ρ trajectory. In the case of π^0, on the contrary, ω (ρ) contributes only to the isovector (isoscalar) part of $\hat{t}$.

Using the gauge conditions $\varepsilon^0 = 0$ and $\vec{\varepsilon}_\lambda\cdot\vec{k} = 0$ one obtains the following expression for L and $\vec{K}$ which can be used in any frame of reference:

$$L_\lambda = i\,\frac{G_1}{k}\left(\frac{\vec{P}\cdot(\vec{\varepsilon}_\lambda\times\vec{k}\,)}{2E^-} - \frac{\vec{Q}\cdot(\vec{\varepsilon}_\lambda\times\vec{k}\,)}{2E^+}\right) + i\,\frac{G_1+G_3}{2EE'}\,\vec{Q}\cdot(\vec{\varepsilon}_\lambda\times\vec{P}\,) + i\,\frac{G_4}{2EE'}\,\vec{Q}\cdot(\vec{k}\times\vec{P}\,), \tag{13a}$$

$$\vec{K}_\lambda = \vec{\varepsilon}_\lambda\left[-G_1 + G_3 + \frac{G_1}{2k}\,\vec{k}\cdot\left(\frac{\vec{P}}{E^+} - \frac{\vec{Q}}{E^-}\right) - \frac{G_1+G_3}{4EE'}\left(P^2 - Q^2\right)\right] + \vec{k}\left[-\frac{G_1}{2k}\,\vec{\varepsilon}_\lambda\cdot\left(\frac{\vec{P}}{E^+} - \frac{\vec{Q}}{E^-}\right) - G_4\left(\frac{P^2-Q^2}{4EE'} - 1\right)\right] + \vec{P}\left[-\frac{G_4}{2}\left(\frac{k}{E^+} - \frac{\vec{k}\cdot\vec{P}}{EE'}\right) + \frac{G_2}{2E^-} + \frac{G_1+G_3}{2EE'}\,\vec{\varepsilon}_\lambda\cdot\vec{P}\right] + \vec{Q}\left[\frac{G_4}{2}\left(\frac{k}{E^-} - \frac{\vec{k}\cdot\vec{Q}}{EE'}\right) - \frac{G_2}{2E^+} - \frac{G_1+G_3}{2EE'}\,\vec{\varepsilon}_\lambda\cdot\vec{Q}\right], \tag{13b}$$

where

$$\vec{Q} = \vec{k} - \vec{q}, \quad \vec{P} = \vec{p} + \vec{p}\,', \quad E = E_i + M_N,$$
$$E' = E_f + M_N, \quad \frac{1}{E^+} = \frac{1}{E} + \frac{1}{E'}, \quad \frac{1}{E^-} = \frac{1}{E} - \frac{1}{E'}. \tag{14}$$

The amplitudes G_i, $i = 1,\ldots,4$, are expressed in terms of the invariant amplitudes A_i as

$$G_1 = NN'kA_1, \quad G_2 = NN'A_2(\vec{\varepsilon}_\lambda\cdot\vec{Q}\,k^\mu P_\mu - \vec{\varepsilon}_\lambda\cdot\vec{P}\,k^\mu Q_\mu),$$
$$G_3 = NN'A_3\,k^\mu P_\mu, \quad G_4 = NN'A_3\,\vec{\varepsilon}_\lambda\cdot\vec{P} \tag{15}$$

with $Q_\mu = k_\mu - q_\mu$, $P_\mu = p_\mu + p'_\mu$, $N = \sqrt{E/2M_N}$, $N' = \sqrt{E'/2M_N}$. In the expressions for G_3 and G_4 in Eq. (15) I have explicitly taken into account the equality $A_3 = A_4$ [see Eq. (8)].

Equations (13) are equivalent to Eqs. (35) of Ref. [12], except for an erroneous minus sign of G_2 in the last line in Eq. (35b). When the operator $\hat{t}_{\eta\gamma}$ is embedded into the nuclear amplitude in the peripheral region (the energy and momentum transferred to the nucleus are small), the main contribution is provided by the small nuclear momenta $\vec{p}$ and $\vec{p}\,'$. In this case, in Eqs. (13) one can neglect the terms proportional to $1/E^-$ and $G_4/(EE')$.

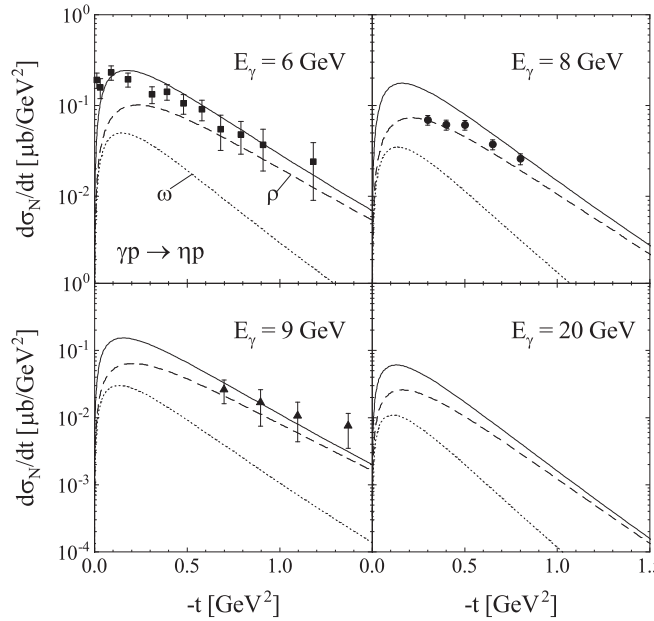

FIG. 1. Differential cross section for $\gamma p \to \eta p$. The curves are the Regge model calculation with parameters taken from Ref. [15]. By the dashed (dotted) lines the separate contribution of ρ (ω) is shown. Data are from [16] (circles), [17] (squares), and [18] (triangles).

The invariant differential cross section for $\gamma p \to \eta p$,

$$\frac{d\sigma_N}{dt} = \frac{M_N^2}{8\pi\left(s - M_N^2\right)^2}\sum_{\lambda=\pm1}[|L_{\lambda(0)} + L_{\lambda(1)}|^2 + |\vec{K}_{\lambda(0)} + \vec{K}_{\lambda(1)}|^2], \tag{16}$$

is presented in Fig. 1 at several photon energies. At the extreme forward angles $\theta \to 0$ where $\vec{P} \parallel \vec{Q}$, Eqs. (13) reduce to

$$L_\lambda \approx 0,$$
$$\vec{K}_\lambda \approx \vec{\varepsilon}_\lambda\,(G_1 - G_3) \sim \frac{t}{(2M_N)^2} \ll 1, \tag{17}$$

so that the cross section rapidly decreases. Furthermore, as one can see, the predicted cross section has a predominantly isovector character. The ratio of the ρ to ω contributions is about 2.5 at maximum and increases with increasing angle. Because of this dominance of the isovector part I expect enhancement of the nuclear transitions to the $T = 1$ states in ^{12}C (as well as in other isospin-zero nuclei), in particular, those leading to excitation of the giant dipole resonance.

III. NUCLEAR PHOTOPRODUCTION

I consider the nuclear reaction

$$\gamma(k^\mu, \lambda) + A_i\left(Q_i^\mu\right) \to \eta(q^\mu) + A_f\left(Q_f^\mu\right), \tag{18}$$

TABLE I. The $1p$ levels of ^{12}C with spin-parity J^π, isospin T, and excitation energy ϵ taken into account in the present calculation.

Level No.	J^π	T	ϵ [MeV]
1	0^+	0	0.00
2	2^+	0	4.43
3	1^+	0	12.73
4	1^+	1	15.11
5	2^+	1	16.11

where the nucleus goes over from the initial state $|J_iM_i;T_iM_{T_i}\rangle$ into the final state $|J_fM_f;T_fM_{T_f}\rangle$. The latter may coincide with the initial state (coherent channel) or be one of the excited states belonging to the discrete spectrum. The four-momenta of the participating particles are

$$k^\mu = (E_\gamma, \vec{k}\,), \quad Q_i^\mu = (E_i, \vec{Q}_i\,),$$
$$q^\mu = (\omega_\eta, \vec{q}\,), \quad Q_f^\mu = (E_f, \vec{Q}_f). \tag{19}$$

The differential cross section,

$$\frac{d\sigma}{d\Omega} = \mathcal{K}\,\frac{\mathcal{F}_{\rm c.m.}}{2(2J_i+1)}\sum_{\lambda M_i M_f}|\langle A_f;\eta|\hat{T}|A_i;\gamma\rangle|^2, \tag{20}$$

is determined by the transition matrix element

$$\langle A_f;\eta|\hat{T}|A_i;\gamma\rangle \equiv \langle J_fM_f;T_fM_{T_f};\eta(\vec{q}\,)|\hat{T}|J_iM_i;T_iM_{T_i};\gamma(\vec{k};\lambda)\rangle. \tag{21}$$

The factor $\mathcal{F}_{\rm c.m.}$ is introduced to effectively take into account the lack of translational invariance of the shell model. I use the standard expression, corresponding to zero oscillations of the nuclear center of mass,

$$\mathcal{F}_{\rm c.m.} = e^{(r_0Q)^2/2A} \tag{22}$$

with $\vec{Q} = \vec{k} - \vec{q}$, where r_0 is the oscillator parameter and A the nuclear mass number.

All calculations are performed in the center-of-mass (c.m.) frame. The relevant phase space factor reads

$$\mathcal{K} = \frac{q}{k}\frac{E_iE_f}{(4\pi W)^2}, \tag{23}$$

where W is the total energy. I use nonrelativistic normalization of the initial and final nuclear states. The differential cross section in the laboratory frame is calculated from Eq. (20) with the appropriate Jacobian $J = |d\Omega_{\rm c.m.}/d\Omega_{\rm lab}|$.

A. Coherent photoproduction and excitation of low-ling discrete levels

For the coherent channel as well as for natural parity transitions to low-lying levels occurring within the $1p$ shell ($1p \to 1p$) I apply the intermediate coupling shell model of Ref. [19]. The corresponding excitation levels of ^{12}C known from experiment are listed in Table I.

For the basic single-particle states one uses in [19] the wave functions from the independent particle shell model with harmonic oscillator potential. Their radial part is determined by the orbital momentum l only, so that it is convenient to develop the formalism within the LS-coupling scheme. In this case, the totally antisymmetric wave function for the nuclear configuration with a closed $1s$ shell core and $A-4$ nucleons in the outer $1p$ shell is

$$\Psi(JM;TM_T) = \sum_{[\lambda]LS}\alpha^{JT}_{[\lambda]LS}\sum_{M_LM_S}C^{JM}_{LM_L\,SM_S}\Phi([\lambda]LM_L\,SM_S;TM_T), \tag{24}$$

where $C^{JM}_{LM_L\,SM_S}$ is the usual Clebsch-Gordan coefficient, and $\alpha^{JT}_{[\lambda]LS}$ determines the weight of a pure configuration $\Phi([\lambda]LM_L\,SM_S;TM_T)$ of given orbital momentum L, spin S, and the Young tableau $[\lambda]$. The values of $\alpha^{JT}_{[\lambda]LS}$ for different $1p$-shell nuclei are given in [19]. By the use of fractional parentage coefficients I can write

$$\Phi([\lambda]LM_L\,SM_S;TM_T) = \sum_{[\lambda']L'S'T'}\langle(1p)^{A-4}\,[\lambda]\,LST|\}\,(1p)^{A-5}\,[\lambda']L'S'T'\rangle \times [\,\psi([\lambda']L'S'T')\otimes\phi_{1p}\,]^{LST}_{M_LM_SM_T}, \tag{25}$$

where $\psi([\lambda']L'S'T')$ is the wave function of the $(1p)^{A-5}$ configuration and ϕ_{1p} is the wave function of a single nucleon on the $1p$ shell. For the ^{12}C oscillator range parameter, I used the standard value

$$r_0 = 1.64\,\text{fm}. \tag{26}$$

To take into account the energy and momentum dependence of the single-nucleon amplitude $\hat{\imath}_{\eta\gamma}$ as given by Eqs. (13) I calculate the transition matrix element in Eq. (20) in momentum space, rather than in coordinate space. The corresponding formalism is described in detail in [12,20].

Using Eqs. (24) and (25) in Eq. (21), one obtains for the squared matrix element

$$\frac{1}{2J_i+1}\sum_{M_iM_f}|\langle J_fM_f;T_fM_{T_f};\eta(\vec{q}\,)|\hat{T}|J_iM_i;T_iM_{T_i};\gamma(\vec{k},\lambda)\rangle|^2 = \sum_{JM}|F_{JM}(\vec{q};\vec{k},\lambda)|^2 \tag{27}$$

with

$$F_{JM} = 4\delta_{J0}\delta_{M0}F^{(1s)} + (A-4)F^{(1p)}_{JM}. \tag{28}$$

Here, I add the $1s$-shell term proportional to $F^{(1s)}$, which gives rise only to the coherent channel. The second term corresponding to the partial transitions of the type $1p \to 1p$, can be presented in the form

$$F^{(1p)}_{JM}(\vec{q};\vec{k},\lambda) = \sum_{LST}(-1)^{L+T}\hat{L}\hat{S}\hat{T}\,C^{T_fM_{T_f}}_{T_iM_{T_i}TM_{T_f}-M_{T_i}}\,\mathcal{B}_{JLST}\,I^{LST}_{JM}(\vec{q};\vec{k},\lambda), \tag{29}$$

where $\hat{j} \equiv \sqrt{2j+1}$. The coefficients $\mathcal{B}_{JLST}$ are determined by the quantum numbers of the transition $|J_i M_i; T_i M_{T_i}\rangle \to |J_f M_f; T_f M_{T_f}\rangle$:

$$\mathcal{B}_{JLST} = 2\hat{J}_f \hat{T}_i \sum_{[\lambda_i] L_i S_i} \sum_{[\lambda_f] L_f S_f} (-1)^{L_f+S_f+T_f} \hat{L}_i \hat{S}_i \hat{L}_f \hat{S}_f \begin{Bmatrix} J & J_i & J_f \\ S & S_i & S_f \\ L & L_i & L_f \end{Bmatrix} \alpha^{J_i T_i}_{[\lambda_i] L_i S_i} \alpha^{J_f T_f}_{[\lambda_f] L_f S_f}$$

$$\times \sum_{[\lambda'] L' S' T'} (-1)^{1+L'+S'+T'} \langle (1p)^{A-4} [\lambda_i] L_i S_i T_i | \} (1p)^{A-5} [\lambda'] L' S' T' \rangle$$

$$\times \langle (1p)^{A-4} [\lambda_f] L_f S_f T_f | \} (1p)^{A-5} [\lambda'] L' S' T' \rangle \begin{Bmatrix} 1 & L & 1 \\ L_f & L' & L_i \end{Bmatrix} \begin{Bmatrix} \frac{1}{2} & S & \frac{1}{2} \\ S_f & S' & S_i \end{Bmatrix} \begin{Bmatrix} \frac{1}{2} & T & \frac{1}{2} \\ T_f & T' & T_i \end{Bmatrix}, \tag{30}$$

whereas the integral $I^{LST}_{JM}(\vec{q}; \vec{k}, \lambda)$ given by

$$I^{LST}_{JM}(\vec{q}; \vec{k}, \lambda) = \int \phi^*_{1p}(p') \chi^{(-)*}_{\vec{q}}(\vec{q}\,') \left[[Y^1(\hat{p}\,') \otimes Y^1(\hat{p})]^L \otimes K^S_{\lambda(T)}(\vec{p}, \vec{q}\,') \right]^J_M \phi_{1p}(p) \frac{d^3p}{(2\pi)^3} \frac{d^3q'}{(2\pi)^3} \tag{31}$$

with $\vec{p}\,' = \vec{k} + \vec{p} - \vec{q}\,'$ is basically determined by the dynamical properties of the photoproduction process.

In Eq. (31), $\phi_{1p}(p)$ is the 'radial' part of the single particle wave function in momentum space

$$\phi_{1pm}(\vec{p}\,) = \phi_{1p}(p) Y_{1m}(\hat{p}). \tag{32}$$

In the harmonic oscillator shell model

$$\phi_{1p}(p) = 4\pi \sqrt{\frac{4}{3}\sqrt{\pi} r_0^3}\, (pr_0)\, e^{-(pr_0)^2/2}. \tag{33}$$

I use the normalization condition

$$\int |\phi_{1p}(\vec{p}\,)|^2 \frac{d^3p}{(2\pi)^3} = 1. \tag{34}$$

The function $\chi^{(-)}_{\vec{q}}(\vec{q}\,')$ entering the integrand in Eq. (31) describes the emitted meson interacting with the target nucleus.

The amplitudes $K^S_{\lambda(T)}$ are defined by representation of the operator (11) in terms of tensor products

$$L_{\lambda(T)} + \vec{K}_{\lambda(T)} \cdot \vec{\sigma} = \sum_{S=0,1} \sum_{\mu=-S}^{S} (-1)^\mu K^S_{-\mu,\lambda(T)} \sigma^S_\mu \tag{35}$$

with $\sigma^0 = 1$, $\sigma^1_\mu = \sigma_\mu$.

For the $1s$-shell term in Eq. (28) which contributes to the coherent $E0$ transition only, I will have

$$F^{(1s)}(\vec{q}; \vec{k}, \lambda) = \frac{1}{4\pi} \int \phi^*_{1s}(p') \phi_{1s}(p) \times \chi^{(-)*}_{\vec{q}}(\vec{q}\,') K^0_{\lambda(0)} \frac{d^3p}{(2\pi)^3} \frac{d^3q'}{(2\pi)^3}. \tag{36}$$

Here, the 'radial' part of the $1s$-shell nucleon wave function reads

$$\phi_{1s}(p) = 4\pi \sqrt{2\sqrt{\pi} r_0^3}\, e^{-(pr_0)^2/2}. \tag{37}$$

In the coherent channel, when the initial and the final nuclear states coincide, a good approximation is provided by factorization of the matrix element (31) in which the elementary operator $K^S_{\mu,\lambda(T)}$ is taken out of the integral over the struck nucleon momentum $\vec{p}$ at an effective value $\langle \vec{p}\, \rangle$, determined by (in the γA c.m. frame)

$$\langle \vec{p}\, \rangle = -\frac{1}{A} \vec{k} - \frac{A-1}{2A} \left(\vec{k} - \vec{q} \right). \tag{38}$$

Neglecting also the influence of the difference between $\vec{q}\,'$ and the asymptotic meson momentum $\vec{q}$ one can further frees $K^S_{\mu,\lambda(T)}$ at $\vec{q}\,' = \vec{q}$ to get, in the general case,

$$I^{LST}_{JM}(\vec{q}; \vec{k}, \lambda) = \sum_{M_L \mu} C^{JM}_{LM_L S\mu} K^S_{\mu,\lambda(T)}(\langle \vec{p}\, \rangle, \vec{q}) \int \phi^*_{1p}(p') \chi^{(-)*}_{\vec{q}}(\vec{q}\,') [Y^1(\hat{p}') \otimes Y^1(\hat{p})]^L_{M_L} \phi_{1p}(p) \frac{d^3p}{(2\pi)^3} \frac{d^3q'}{(2\pi)^3}. \tag{39}$$

The validity of this approximation for transitions with different sets of transferred momenta J, L, S, T was considered in rather detail, e.g., in [20].

Note that the factorization (39) is widely used in calculation of the coherent amplitude in coordinate-space representation. In the elementary operator one usually takes into account only the dominant spin-independent part proportional to $\vec{q} \cdot (\vec{k} \times \vec{\varepsilon}_\lambda)$, so that the factorization with respect to the nucleon momentum $\vec{p}$ becomes trivial. At the same time, there is no guarantee that the dependence of $K^S_{\mu,\lambda(T)}$ on $\vec{q}\,'$ does not affect the value of the integral (31). Moreover, as will be shown below, even in the coherent channel, which is the least affected by model uncertainties, this dependence is significant.

B. Excitation of higher lying $T = 1$ levels

To calculate the partial transitions in which the nucleus is excited to the levels above the $1p$ shell, in particular those involving parity change, I use, for the nuclear structure inputs, the phenomenological transition form factors from Ref. [21]. The latter were obtained by fitting electron scattering data within the generalized Helm model and were also applied to charged pion photoproduction on nuclei in [22,23]. In order to obtain a suitable expression for my amplitude (21), I neglect the meson-nuclear interaction in the final state and use the factorization approximation Eqs. (39) and (38). The resulting expression for a transition from the initial state $J_i = T_i = 0$ reads, in coordinate space,

$$\begin{aligned}
&\langle A_f;\eta|\hat{T}|A_i;\gamma\rangle \\
&\quad= \big\langle J_f M_f; T_f M_{T_f}\big|\sum_{i=1}^{A}\hat{t}_{\eta\gamma}(i)e^{\vec{Q}\cdot\vec{r}_i}|0;0\rangle \\
&\quad= 4\pi\sum_{LS} i^L(-1)^{L+S-J_f+M_f}\big[Y^L(\hat{Q})\otimes K^S_{\lambda(T_f)}\big]^{J_f}_{-M_f} \\
&\qquad\times\langle J_f T_f \parallel j_L(Qr)[Y^L(\hat{r})\otimes\sigma^S]^{J_f}\parallel 00\rangle, \qquad (40)
\end{aligned}$$

where $\vec{Q} = \vec{k} - \vec{q}$, and $K^S_{\lambda(T)}$ is calculated at $\vec{p} = \langle\vec{p}\,\rangle$ given by Eq. (38). Here, I consider only the transitions to the isotriplet states, $T_f = 1$. The reduced matrix elements appearing in Eq. (40) are directly related to the transition form factors $I_L(Q)$ and $I_{LL'}(Q)$ from [21], determined by the multipole expansion of the spin-independent and the spin-flip matrix elements:

$$\begin{aligned}
&\langle J_f M_f|\frac{1}{2}\sum_{i=1}^{A}\tau_{0i}\,e^{i\vec{Q}\cdot\vec{p}_i}|J_i M_i\rangle \\
&\quad= \frac{4\pi}{\hat{J}_f}\sum_{LM} C^{J_f M_f}_{J_i M_i LM} I_L(Q) Y^*_{LM}(\hat{Q}), \qquad (41a)\\
&\langle J_f M_f|\frac{1}{2}\sum_{i=1}^{A}\vec{\sigma}_i\tau_{0i}\,e^{i\vec{Q}\cdot\vec{p}_i}|J_i M_i\rangle \\
&\quad= \frac{4\pi}{\hat{J}_f}\sum_{L'LM} C^{J_f M_f}_{J_i M_i LM} I_{LL'}(Q)\vec{Y}^*_{LL'M}(\hat{Q}). \qquad (41b)
\end{aligned}$$

Taking into account the spin-isospin structure of the operator $\hat{t}_{\eta\gamma}$ (13), a direct comparison with Eq. (41) gives, for the reduced matrix elements,

$$\begin{aligned}
\langle J_f 1\|j_{J_f}(Qr)[Y^{J_f}(\hat{r})\otimes\sigma^0]^{J_f}\|00\rangle &= i^{-J_f}\frac{2}{\hat{J}_f} I_{J_f}(Q),\\
\langle J_f 1\|j_L(Qr)[Y^L(\hat{r})\otimes\sigma^1]^{J_f}\|00\rangle &= i^{-L}\frac{2}{\hat{J}_f} I_{J_f L}(Q). \qquad (42)
\end{aligned}$$

Application of the generalized Helm model [21] leads to a parametrization of the relevant transition form factors of the form

$$\begin{aligned}
I_L(Q) &= \beta_L e^{-\frac{1}{2}(gQ)^2} j_L(QR),\\
I_{LL'}(Q) &= \overline{\gamma}_{LL'} e^{-\frac{1}{2}(gQ)^2} j_{L'}(Q\overline{R}). \qquad (43)
\end{aligned}$$

The parameters g, β_J, R, $\overline{\gamma}_{JL}$, and $\overline{R}$ were obtained in [21] by fitting the data for inelastic electron scattering on ^{12}C to $T = 1$ states. Table II lists the corresponding levels which were taken into account in the present calculation.

TABLE II. Enumeration of the $T = 1$ levels of ^{12}C included in the present calculation. The level No.12 is the collective strength of the giant electric dipole resonance states over the 21–26 MeV region.

Level No.	J^π	T	ϵ [MeV]
1	2^-	1	16.58
2	1^-	1	17.23
3	1^-	1	18.15
4	3^-	1	18.72
5	2^+	1	18.81
6	1^-	1	19.20
7	2^-	1	19.40
8	4^-	1	19.60
9	2^+	1	20.00
10	3^+	1	20.60
11	3^-	1	21.60
12	1^-	1	21–26

C. Final state interaction

To calculate the matrix element I^{LST}_{JM} (31) I need the meson wave function in the momentum space $\chi^{(-)*}_{\vec{q}}(\vec{q}\,')$. It can be expressed in terms of the meson-nuclear T-matrix $T_{\eta A}$ as

$$\begin{aligned}
\chi^{(-)*}_{\vec{q}}(\vec{q}\,') &= \chi^{(+)}_{\vec{q}}(\vec{q}\,')\\
&= (2\pi)^3\delta(\vec{q}-\vec{q}\,') + \frac{T_{\eta A}(\vec{q},\vec{q}\,')}{E(q)-E(q')+i\epsilon} \qquad (44)
\end{aligned}$$

with $E(q) = W$ and $E(q') = \sqrt{q'^2 + M_\eta^2} + \sqrt{q'^2 + M_A^2}$.

Inserting Eq. (44) into the matrix element (31), I obtain (the indices are dropped for the moment)

$$I(\vec{q},\vec{k}\,) = I_{PW}(\vec{q},\vec{k}\,) + I_{\eta A}(\vec{q},\vec{k}\,), \qquad (45)$$

where the plane-wave matrix element $I^{PW}(\vec{q},\vec{k})$ is given by Eq. (31) with $\chi^{(-)*}_{\vec{q}}(\vec{q}\,') \to (2\pi)^3\delta(\vec{q}-\vec{q}\,')$ and the second term reads

$$I_{\eta A}(\vec{q},\vec{k}\,) = \int \frac{T_{\eta A}(\vec{q},\vec{q}\,')\,I_{PW}(\vec{q}\,',\vec{k}\,)}{E(q)-E(q')+i\epsilon}\,\frac{d^3q'}{(2\pi)^3}. \qquad (46)$$

For the off-shell T matrix

$$T_{\eta A}(\vec{q},\vec{q}\,') = \int e^{-i\vec{q}\,'\cdot\vec{r}}\,V_{\eta A}(\vec{r}\,)\,\chi^{(+)}_{\vec{q}}(\vec{r}\,)\,d^3r \qquad (47)$$

I use the eikonal approximation, in which $\chi^{(+)}_{\vec{q}}(\vec{r}\,)$ is given by

$$\chi^{(+)}_{\vec{q}}(\vec{r}\,) = \exp\left[i\vec{q}\cdot\vec{r} - \frac{i}{\beta_\eta}\int_{-\infty}^{0} V_{\eta A}(\vec{r}+\hat{q}s)\,ds\right]. \qquad (48)$$

Following earlier work, I assume that in the interaction of a fast meson with a nucleus, only the absorptive part is important, and take the relevant optical potential $V_{\eta A}(r)$ purely imaginary having the shape of a square well with radius R

($R = 1.3\,A^{1/3}$ fm):

$$V_{\eta A}(\vec{r}\,) = \begin{cases} -V_0, & r < R, \\ 0, & r \geqslant R. \end{cases} \tag{49}$$

For the depth V_0 I apply the Rayleigh approximation

$$V_0 = 2\pi\,\frac{\beta_\eta}{q}\,\rho_A f_{\eta N}(0) = i\frac{\beta_\eta}{2\lambda}, \tag{50}$$

where $\beta_\eta = q/\omega_\eta$, $\rho_A = A/(4\pi R^3/3)$ is the nuclear density, and $f_{\eta N}(0)$ is the elastic ηN scattering amplitude in the forward direction. The mean free path λ is related to the total ηN scattering cross section as

$$\lambda = \frac{1}{\rho_A \sigma_{\eta N}}. \tag{51}$$

For $\sigma_{\eta N}$ I take

$$\sigma_{\eta N} = \tfrac{1}{2}(\sigma_{\pi^+ p} + \sigma_{\pi^- p}) \approx 23\,\text{mb}. \tag{52}$$

Using cylindrical coordinates with the z axis along the asymptotic momentum $\vec{q}$, one obtains

$$T_{\eta A}(\vec{q}, \vec{q}\,') = -i\beta_\eta\gamma \int_0^R e^{-\gamma\sqrt{R^2-\rho^2}}\,\rho\,d\rho \int_0^{2\pi} e^{-iq'_\perp \rho\cos\phi} d\phi \times \int_{-\sqrt{R^2-\rho^2}}^{\sqrt{R^2-\rho^2}} e^{(i(q-q'_\parallel)-\gamma)z} dz \tag{53}$$

with $\gamma = (2\lambda)^{-1}$, which after integration over ϕ and z and the substitution $y = \sqrt{1-(\rho/R)^2}$ reduces to

$$T_{\eta A}(\vec{q}, \vec{q}\,') = -i\frac{4\pi\gamma\beta_\eta R^2}{q - q'_\parallel + i\gamma} \int_0^1 J_0(q'_\perp R\sqrt{1-y^2}) e^{-\gamma R y} \times \sin[(q - q'_\parallel + i\gamma)Ry]\,y\,dy, \tag{54}$$

where

$$q'_\parallel = \frac{1}{q}(\vec{q}\,' \cdot \vec{q}\,), \quad q'_\perp = \frac{1}{q}\sqrt{(q'q)^2 - (\vec{q}\,' \cdot \vec{q}\,)^2}. \tag{55}$$

Integration in Eq. (46) was carried out using the standard representation of the Green's function:

$$\frac{1}{E(q) - E(q') + i\epsilon} = \frac{P}{E(q) - E(q')} - i\pi\,\delta(E(q) - E(q')). \tag{56}$$

At high energies, to which my calculation is restricted, the product $T_{\eta A}(\vec{q}, \vec{q}\,')\,I_{PW}(\vec{q}\,', \vec{k}\,)$ in the integrand has very sharp maximum at $\vec{q}\,' \approx \vec{k} \approx \vec{q}$. Therefore, the main contribution to the integral comes from the first term in Eq. (56). Retaining only this term Eq. (46) is reduced to a simple two-dimensional integral

$$I_{\eta A}(\vec{q}, \vec{k}\,) \approx i\frac{q}{4\pi} \int f_{\eta A}(\theta_{q'}) I_{PW}(\vec{q}\,', \vec{k}\,)\,d\Omega_{q'}, \tag{57}$$

where $q' = q$. The scattering amplitude for azimuthally symmetric potential is given by the well-known expression

$$f_{\eta A}(\theta) = iq \int_0^\infty J_0(qb)[1 - e^{i\chi(b)}]\,b\,db \tag{58}$$

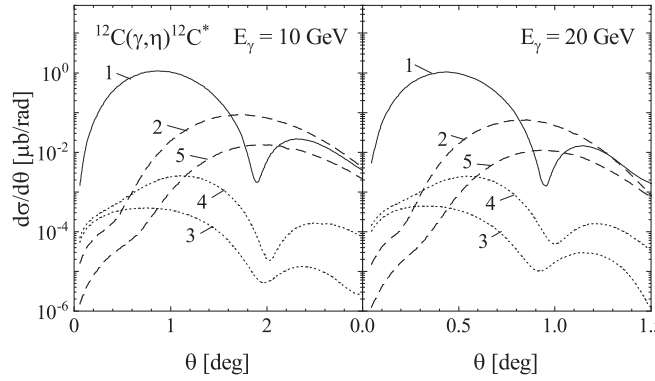

FIG. 2. Differential cross section for $^{12}\text{C}(\gamma, \eta)\,^{12}\text{C}^*$ in the laboratory frame with excitation of the $1p$-shell levels at two photon energies. The levels are enumerated according to Table I.

with the profile function

$$\chi(b) = -\frac{1}{\beta_\eta}\int_{-\infty}^{\infty} V(b + \hat{q}z)dz. \tag{59}$$

In the next section, the cross section calculated in the approximation (57) is compared to that obtained with inclusion of both terms in the Green's function (56).

IV. RESULTS AND DISCUSSION

In Figs. 2 and 3 I show the differential cross section

$$\frac{d\sigma}{d\theta} = 2\pi\,\sin\theta\,\frac{d\sigma}{d\Omega}, \tag{60}$$

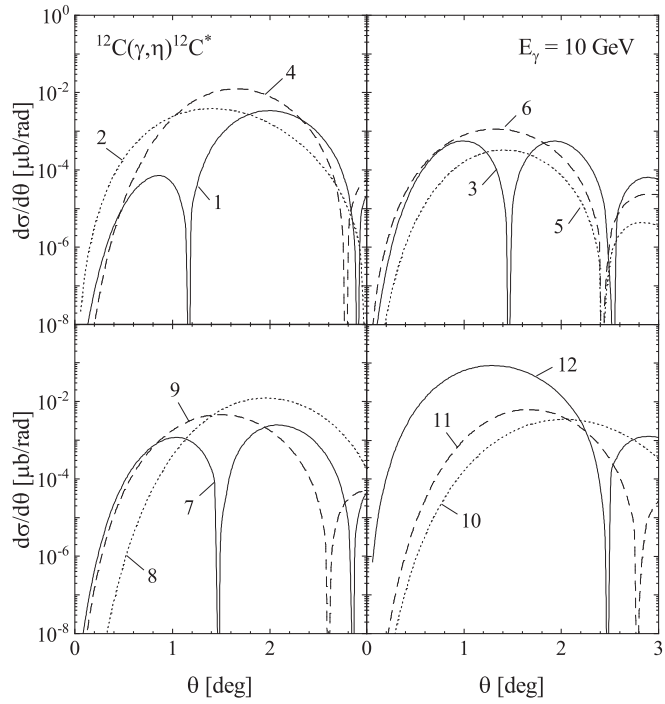

FIG. 3. Differential cross section for $^{12}\text{C}(\gamma, \eta)^{12}\text{C}^*$ with excitation of the $T = 1$ states at $E_\gamma = 10$ GeV. Enumeration of the levels is given in Table II.

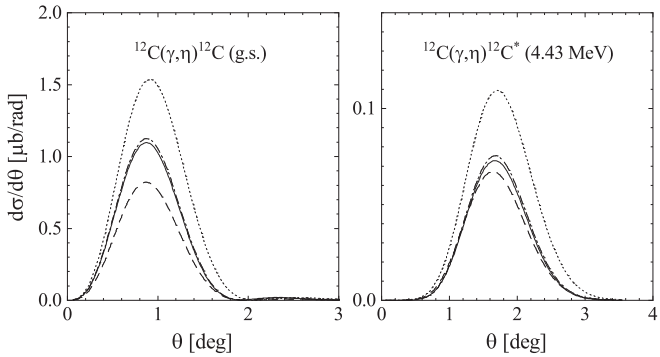

FIG. 4. Differential cross section for coherent (left panel) and incoherent η photoproduction with excitation of the level $2^+;0$ (4.43 MeV). Incident laboratory photon energy E_γ is 10 GeV. The dotted curves show the plane-wave calculations. The solid curves are the full calculations including final state interaction as described in Sec. C. In the dash-dotted curves only the second term in the Green's function (56) is retained. The dashed curves are obtained within the factorization approximation (39).

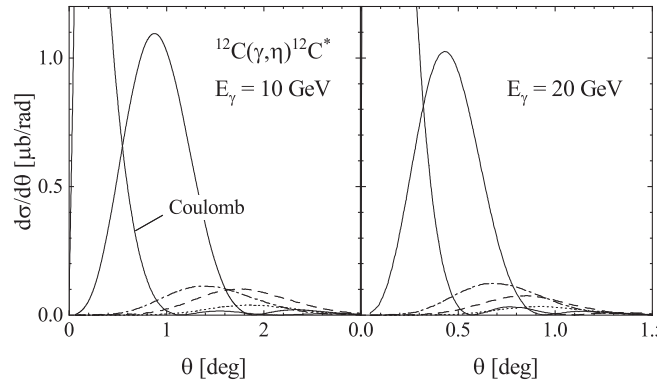

FIG. 5. Various contributions to the differential cross section for $^{12}\mathrm{C}(\gamma,\eta)\,^{12}\mathrm{C}^*$: coherent (solid curve), sum of the $1p$-shell excitations listed in Table I (dashed curve), sum of the $T=1$ transitions to higher levels, Table II (dash-dotted curve), $3^-;0$ (9.63 MeV) level (dotted curve). The leftmost curve shows the Coulomb (Primakoff) cross section. The interference between the Coulomb and the coherent production amplitude is not included.

for the reaction $^{12}\mathrm{C}(\gamma,\eta)\,^{12}\mathrm{C}^*$ in the laboratory frame. As expected, the coherent channel provides the dominant contribution. The model independent approximation (1) gives for the η angle $\theta_\mathrm{C}^{\max}$, at which the coherent cross section reaches maximum, the value

$$\theta_\mathrm{C}^{\max}=\frac{3}{\sqrt{5}E_\gamma\langle r^2\rangle^{1/2}}. \tag{61}$$

Taking for the ^{12}C rms radius $\langle r^2\rangle^{1/2}=2.4$ fm I obtain $\theta_\mathrm{C}^{\max}=0.63^\circ$ and 0.32° for $E_\gamma=10$ and 20 GeV, respectively, slightly to the left of the coherent peak seen in Fig. 2. Direct calculations show that the difference comes from additional dependence of the isoscalar spin-independent amplitude $K^0_{\lambda(0)}$ on θ [in addition to the trivial $\sin\theta$ dependence of the product $\vec{q}\cdot(\vec{k}\times\vec{\varepsilon}_\lambda)$].

The angular dependence of the inelastic cross sections, as well as their maximum value and positions of the maxima, are of course determined by the type of the corresponding transitions. Among the low-lying states belonging to a discrete spectrum, the $E2$ level $2^+;0$ (4.43 MeV) (level 2 in Table I) shows up most strongly.

As for the transitions to higher-lying states with $T=1$ (Fig. 3), here, only the group of levels forming a giant $E1$ resonance in the energy range 21–26 MeV (level 12 in Table II) makes a more or less noticeable contribution. The role of other transitions remains limited. I should emphasize that the calculations in Fig. 3 were performed without taking into account meson-nuclear interaction. This, in particular, leads to very deep minima $d\sigma/d\theta=0$, in contrast to the less pronounced diffractive structure in Fig. 2. In view of this approximate treatment, to which I have to resort in order to express the amplitude in terms of the phenomenological transition form factors as given by Eqs. (40) to (43), my results in Fig. 3 should be regarded to some extent as estimates.

In Fig. 4 I demonstrate influence of some commonly used approximations. First of all, I note that the factorization approximation (39) is rather crude. In particular, it leads to a noticeable overestimation of the suppression effect due to the meson absorption. Note that it is the replacement $\vec{q}\,'\to\vec{q}$ in the elementary amplitude $K^S_{\mu,\lambda(T)}$ which causes the main error due to factorization, while the substitution $\vec{p}\to\langle\vec{p}\,\rangle$ has a negligible effect on the result. Also noteworthy is the good quality of the on-shell approximation (57), in which only the pole term is taken into account in the Green's function (56).

The above conclusions only apply to the dominant transitions presented in Fig. 4. As straightforward calculations show, in other channels (3, 4, and 5 in Table I), which are more sensitive to the details of the nuclear structure, the contribution of the first term in the formula (56) turns out to be quite significant and must necessarily be taken into account. The same applies to the local approximation $\vec{p}\to\langle\vec{p}\,\rangle$ (38), which leads to a large error in the calculation of these transitions.

The relative importance of inelastic channels is additionally demonstrated in Fig. 5. Noteworthy is the relatively large contribution of $T=1$ transitions (dash-dotted curve) dominated by excitation of the giant $E1$ resonance (see Fig. 3). This is at least partially explained by the predominantly isovector character of η photoproduction in my model due to the dominance of ρ-meson exchange (see Fig. 1).

Here, I also show the cross section for the $E3$ transition to the $3^-;0$ (9.63 MeV) level (dotted curve). The latter is accompanied by the parity change, so it cannot be attributed to the $0\hbar\omega$ excitation of the type $1p\to1p$. For calculations, the $3^-;0$ level was assumed to be a purely particle-hole $(1p_{3/2})^{-1}1d_{5/2}$ state. Since such a naive model is known to give a too large cross section (see, e.g., [24]), the corresponding amplitude was additionally multiplied by a damping factor ξ. The value $\xi=0.38$ was adjusted in such a way that by substituting $\hat{t}_{\eta\gamma}=1$ (that is, $K^0_{\lambda(0)}=1$, $K^0_{\lambda(1)}=K^1_{\lambda(T)}=0$) the averaged squared matrix element (27) gives the square of the corresponding longitudinal form-factor for the transition $0^+;0$ (g.s.) $\to3^-;0$ (9.63 MeV) [25].

In the same figures the Coulomb (Primakoff) cross section is also shown for comparison. It was calculated taking

into account meson-nuclear FSI, using the formalism developed in [3]. For the $\eta \to \gamma\gamma$ decay width I used the value $\Gamma_{\eta\to\gamma\gamma} = 0.51$ keV. Note that the Coulomb cross section was computed independently and is presented here only for a clearer demonstration of the importance of other channels. In particular, the results in Fig. 5 do not take into account the interference between the Coulomb and the coherent amplitudes.

On the whole, as we can see from Fig. 5, the resulting contribution of the inelastic channels is rather moderate and amounts to only about 20 % of the coherent one. In addition, the corresponding amplitudes sum up incoherently with the Coulomb amplitude, so that it is probably not very difficult to isolate them in a real data analysis. Thus, one concludes that the dominant part of the inelastic cross section at not very small meson emission angles, which may influence the shape of the Primakoff peak, will be not the transitions to discrete nuclear levels, but quasifree processes with nucleon knockout. A systematic theoretical treatment of the corresponding cross sections is found, for example, in [26,27].

In the present calculation I omitted the influence of the photon shadowing effect, occurring, e.g., in the vector-meson-dominance picture of the photon-hadron scattering. This effect is expected to additionally suppress the cross section. According to [8,9] the resulting differential cross section decreases by about 20% without a noticeable change in the shape.

V. CONCLUSION

I addressed the issue of coherent and incoherent photoproduction of pseudoscalar mesons on p-shell nuclei at high energies in the peripheral region, corresponding to low momentum transfer. One of the main goals of the present work was to examine the role of various inelastic transitions in the immediate vicinity of the Primakoff maximum. This information may appear to be necessary in the analysis of meson photoproduction via the Primakoff effect. Furthermore, in my study, I tried to reduce the uncertainties arising from the traditionally oversimplified treatment of the nuclear structure (closure approximation, neglect of nuclear excitations, use of a uniform nuclear density, etc.).

Assumptions I use in the present study include mainly impulse approximation and classical trajectories of probes in a nucleus for taking into account the meson-nuclear interaction in the final state.

To obtain a reliable description, I apply a relativistic covariant expression for the single-nucleon photoproduction operator. For the nuclear wave functions I adopted a sophisticated intermediate coupling shell model which allowed me to accurately calculate the transitions to individual $0\hbar\omega$ levels.

For the higher discrete levels with $T = 1$ as well as for excitation of the giant resonance states of ^{12}C I used the phenomenological transition form factors obtained in [21] within the generalized Helm model. The main advantage of such an approach is its extreme ease of application. However, the price to be paid for this simplicity is the difficulty of correctly taking into account the nonlocality of the single-nucleon production operator, as well as the influence of the final state interaction (the factorization approximation and plane waves were used).

An important point of my study, which may deserve a criticism, is the uncertainty associated with a treatment of the single-nucleon photoproduction operator. As mentioned in Sec. II, the parameters in Eqs. (8) and (9) taken from [15] were obtained by fitting the differential cross section for $\gamma p \to \eta p$ at photon energies $E_\gamma \leqslant 6$ GeV. In this sense, the calculation presented on the lower right panel of Fig. 1 is, in fact, an extrapolation of the model [15] to higher energies, not limited by any additional physically motivated conditions. Obviously, this uncertainty directly affects the quality of my results for nuclear photoproduction and may be a limiting factor in applying them to the data analysis. Further research in this area requires, first of all, a more reliable analysis of the elementary amplitude, perhaps within a more refined model than the one used in the present study.

ACKNOWLEDGMENTS

The author would like to thank the members of PrimEx Collaboration (L. Gan, A. Gasparian, I. Jaegle, and A. Somov) for numerous fruitful discussions. Financial support for this work was provided by the Russian Science Foundation, Grant No. 22-42-04401.

[1] L. Gan, JPS Conf. Proc. **13**, 020063 (2017).
[2] A. Accardi, P. Achenbach, D. Adhikari, A. Afanasev, C. S. Akondi, N. Akopov, M. Albaladejo, H. Albataineh, M. Albrecht, B. Almeida-Zamora *et al.*, arXiv:2306.09360 [nucl-ex].
[3] C. A. Engelbrecht, Phys. Rev. **133**, B988 (1964).
[4] G. Morpurgo, Nuovo Cimento **31**, 569 (1964).
[5] S. M. Berman, Nuovo Cimento **21**, 1020 (1961).
[6] T. E. Rodrigues, J. D. T. Arruda-Neto, J. Mesa, C. Garcia, K. Shtejer, D. Dale, I. Nakagawa, and P. L. Cole, Phys. Rev. Lett. **101**, 012301 (2008).
[7] G. Fäldt, Nucl. Phys. B **43**, 591 (1972).
[8] S. Gevorkyan, A. Gasparian, L. Gan, I. Larin, and M. Khandaker, Phys. Rev. C **80**, 055201 (2009).
[9] M. M. Kaskulov and U. Mosel, Phys. Rev. C **84**, 065206 (2011).
[10] T. K. Fowler and K. M. Watson, Nucl. Phys. **13**, 549 (1959).
[11] J. D. Bjorken and S. D. Drell, *Relativistic Quantum Mechanics* (McGraw-Hill, New York, 1964).
[12] C. Bennhold and H. Tanabe, Nucl. Phys. A **530**, 625 (1991).
[13] A. Fix and H. Arenhövel, Nucl. Phys. A **620**, 457 (1997).
[14] H. Thom, Phys. Rev. **151**, 1322 (1966).
[15] W. T. Chiang, S. N. Yang, L. Tiator, M. Vanderhaeghen, and D. Drechsel, Phys. Rev. C **68**, 045202 (2003).
[16] J. Dewire, B. Gittelman, R. Loe, E. C. Loh, D. J. Ritchie, and R. A. Lewis, Phys. Lett. B **37**, 326 (1971).
[17] W. Braunschweig, W. Erlewein, H. Frese, K. Luebelsmeyer, H. Meyer-Wachsmuth, D. Schmitz, A. Schultz Von Dratzig, and G. Wessels, Phys. Lett. B **33**, 236 (1970).

[18] R. L. Anderson, D. Gustavson, J. R. Johnson, D. Ritson, B. H. Wiik, W. G. Jones, D. Kreinick, F. V. Murphy, and R. Weinstein, Phys. Rev. D **1**, 27 (1970).
[19] A. N. Boyarkina, Izv. Akad. Nauk SSSR (Ser. Fiz.) **28**, 337 (1964).
[20] L. Tiator and L. E. Wright, Phys. Rev. C **30**, 989 (1984).
[21] H. Überall, B. A. Lamers, J. B. Langworthy, and F. J. Kelly, Phys. Rev. C **6**, 1911 (1972).
[22] F. Cannata, B. A. Lamers, C. W. Lucas, A. Nagl, H. Ueberall, C. Werntz, and F. J. Kelly, Can. J. Phys. **52**, 1405 (1974).
[23] F. J. Kelly, L. J. McDonald, and H. Überall, Nucl. Phys. A **139**, 329 (1969).
[24] J. B. Seaborn, V. Devanathan, and H. Überall, Nucl. Phys. A **219**, 461 (1974).
[25] H. Crannell, Phys. Rev. **148**, 1107 (1966).
[26] T. E. Rodrigues, J. D. T. Arruda-Neto, J. Mesa, C. Garcia, K. Shtejer, D. Dale, I. Nakagawa, and P. L. Cole, Phys. Rev. C **82**, 024608 (2010).
[27] S. Gevorkyan, A. Gasparian, L. Gan, I. Larin, and M. Khandaker, Phys. Part. Nucl. Lett. **9**, 18 (2012).